Quasienergy functions and spectrum for two interacting nonlinear resonances in the region of classical chaos

G. P. Berman, O. F. Vlasova, and F. M. Izraĭlev

Institute of Physics, Siberian Branch of the Academy of Sciences of the USSR, Novisibirsk and Institute of Nuclear Physics, Siberian Branch of the Academy of Sciences of the USSR, Novosibirsk
(Submitted 14 January 1987)

The structure of the quasienergy functions and spectrum is investigated for two interacting nonlinear resonances. Particular attention is devoted to the properties of the quantum system in the case where stochastic motion arises in the classical limit as a result of the overlap of nonlinear resonances. The role of quantum effects in classical chaos is examined.

1. INTRODUCTION

The interaction of highly excited atoms and molecules (Rydberg states) with monochromatic external radiation has recently attracted considerable attention (see, for example, Refs. 1 and 2). Since this concerns the quasiclassical region of population of the levels of a system, in which the anharmonic constant is small, it follows that strong enough excitation will involve a large number of levels in the dynamics of the system. Moreover, a particular form of excitation, analogous to classical stochastic diffusion, may come into play. The mechanism of this diffusion has been extensively studied in classical mechanics and is based on the phenomenon of overlap of nonlinear resonances.[3–5] The dynamics of a quantum-mechanical system during the interaction between a large number of nonlinear resonances has been discussed both in terms of simple models (see, for example, Refs. 4, 6, and 7) and models approaching real systems.[8–10] In these examples, stochasticity arises in a larger region of phase space and can give rise to global instability. At the same time, there are systems in which stochasticity is confined to a relatively small region of phase space. The interaction of two nonlinear resonances, describing, for example, the motion of an electron in the field of two plasma waves[11] is a typical example of this.

The dynamics of the interaction of two nonlinear resonances is studied in Refs. 12 and 13 in the quantum-mechanical case. In particular, it is shown that, when the nonlinear resonances overlap and the quasiclassical parameter is large enough, the behavior of the quantum-mechanical system within finite time intervals is analogous to the stochastic behavior of the corresponding classical system. However, in the course of time, quantum-mechanical effects leading to the suppression of dynamic chaos become significant.[4,6,12,13]

We note that, when the behavior of a nonautonomous quantum-mechanical system is investigated, this can be done in two ways, namely, by studying the dynamics of the system (diffusion, time correlations, and so on) or by analyzing the spectral characteristics (quasienergy spectrum and the structure of quasienergy eigenfunctions[14,15]). While the first of these two approaches has now been satisfactorily developed, the properties of the quasienergy spectrum and, especially, the structure of the eigenfunctions of quantum-mechanical systems that are stochastic in the classical limit, have not been studied to any great extent. On the other hand, in real experiments on the excitation of atoms and molecules in variable fields, the spectral approach is, in some cases,

more natural. It therefore seems to us that, from this point of view, a theoretical investigation of the parameters of the quasienergy spectrum of quantum-mechanical systems with chaotic behavior is now overdue.

In this paper, we report an investigation of the spectral properties of a quantum-mechanical system consisting of two interacting nonlinear resonances. Section 2 gives a description of the model and of the method used in a numerical study of the quasienergy spectrum and quasienergy eigenfunctions. Section 3 discusses the critical region of the perturbation parameter that corresponds in the classical limit to contact between primary resonances. Data are reproduced on the change in the structure of eigenfunctions that accompanies a change in the perturbation parameter. Section 4 investigates the statistical properties of quasienergy eigenfunctions in the region of quantum chaos. Section 5 is devoted to the statistics of the separation between neighboring quasienergy levels as a function of the selection of eigenfunctions according to their localization parameter. The paper concludes with a brief summary.

2. DESCRIPTION OF THE MODEL

As a model that is convenient for studying the interaction between two nonlinear resonances, we take the quantum rotator in the field of two waves:[12,13]

$$\hat{H}=-\gamma\hbar^2\frac{\partial^2}{\partial\theta^2}+V_1\cos(\theta+\nu t)+V_2\cos(\theta-\nu t). \quad (2.1)$$

This Hamiltonian arises, for example, in the analysis of the dipole interaction between an external field (containing two frequencies in resonance with different levels of the unperturbed spectrum) and a nonlinear quantum-mechanical system in the region of quasiclassical population. In this example, γ is the nonlinearity parameter of the unperturbed spectrum, ν is the difference between the resonance frequencies of the external field, and $V_{1,2}$ are the external-field amplitudes.[12,13]

In the classical limit, the Hamiltonian (2.1) assumes the form

$$H=\gamma I^2+V_1\cos(\theta+\nu t)+V_2\cos(\theta-\nu t), \quad (2.2)$$

where I is the classical action for the system. This Hamiltonian describes the interaction between two nonlinear resonances whose position is defined by

$$\omega(I_1)=2\gamma I_1=-\nu, \quad \omega(I_2)=2\gamma I_2=\nu, \quad (2.3)$$

where $I_{1,2}$ are the resonance values of the action. If we put $V_1 = 0$ (or $V_2 = 0$) in (2.2), the system reduces to the isolated nonlinear resonance, which can be integrated exactly and is characterized by the action width ΔI and the frequency Ω of phase oscillations in the neighborhood of resonance:

$$(\Delta I)_{1,2} = 2(2V_{1,2}/\gamma)^{1/2}, \qquad \Omega_{1,2} = (2\gamma V_{1,2})^{1/2}. \tag{2.4}$$

To describe the interaction between two nonlinear resonances, we introduce their overlap parameter[3]

$$K = [(\Delta I)_1/2 + (\Delta I)_2/2](I_2 - I_1)^{-1} = 2(2\gamma V)^{1/2}/\nu, \tag{2.5}$$

where $V_1 = V_2 = V$. It is readily shown that the parameter K in (2.5) is the only dimensionless parameter that completely determines the dynamics of the classical systems.

When $K \ll 1$, each nonlinear resonance is isolated to a sufficient extent, and the particle cannot leave the region of one resonance for the other. The motion in a large part of phase space is then regular (with the exception of the narrow regions in the neighborhood of the resonance separatrices). A qualitatively new effect occurs when $K \gtrsim 1$, for which the interaction between the resonances becomes significant. The chaotic motion then becomes global in the sense that the stochastic trajectory ceases to belong to the neighborhood of one of the resonances and covers a large region of phase space occupied by the resonances.

The dynamics of (2.2) and the structure of phase space are analyzed in Refs. 3, 16, and 17. Global chaos occurs in the system defined by (2.2) for $K > K_c \simeq 0.71$ (Refs. 16 and 17). Numerical analysis shows that, in the case of well-developed stochasticity, the stochastic region includes large islands that cannot be entered by a stochastic trajectory (for example, when $K \simeq 1.333$), and motion in these islands is stable and regular in character. When K is increased to $K \simeq 4.5$, the large islands break up, and the measure of stable islands inside the stochastic region is found to be small.

We note a significant property of (2.2): large stable regions appear again when K is increased still further. This phenomenon is due to partial overlap of the nonlinear resonances, which results in the shrinking of the region of phase space with stochastic behavior.[5] This behavior of (2.2) for $K \gg 1$ is significantly different from the standard picture,[3] in which an increase in K leads to an increase in the region of phase space occupied by the stochastic component and to an improvement in the stochastic properties of motion.

We now turn to the description of our numerical experiment with the quantum-mechanical model of two interacting nonlinear resonances. We shall introduce dimensionless parameters characterizing the behavior of (2.1). One of these is conveniently taken to be the classical parameter K, given by (2.5), which is independent of $\hbar$. The second dimensionless parameter is purely quantum-mechanical and is defined by

$$\xi = \gamma \hbar T. \tag{2.6}$$

The physical meaning of the latter parameter is as follows.[18] Because (2.2) is a nonlinear system, cells in phase space (I, θ) occupying an action interval of the order of $\Delta I \sim \hbar$ spread out in phase θ during the external-field period $T = 2\pi/\nu$ by an amount of the order of $\Delta\theta \sim (d\omega/dI)/T\Delta I \sim \gamma\hbar T = \xi$. When $\Delta\theta \gtrsim 1$, quantum-mechanical inter-

ference effects become significant even within one period of the motion. In the reverse case, $\xi \ll 1$, quantum-mechanical effects are small, and this condition is the condition for quasiclassical approximation. Moreover, a necessary condition for the validity of quasiclassical behavior is $\delta n \gg 1$, where δn is the characteristic number of levels participating in the dynamics of (2.1) (Refs. 12 and 19). An explicit expression for δn can be introduced in the form of the number of levels in the potential well of an isolated nonlinear resonance, obtained in the quasiclassical approximation for $V_1 = V$, $V_2 = 0$:

$$\delta n = \frac{4}{\pi\hbar}\left(\frac{2V}{\gamma}\right)^{1/2}. \tag{2.7}$$

The behavior of the quantum-mechanical system is thus seen to differ from the classical behavior in that it is determined by three dimensionless parameters, namely, K, ξ, and δn. For example, if we take K and ξ as the independent parameters, we can write

$$\delta n = 4K/\xi. \tag{2.8}$$

From now on, we shall assume that both conditions for quasiclassical behavior are satisfied, namely,

$$\delta n \gg 1 \quad (K \gg \xi), \quad \xi \ll 1, \tag{2.9}$$

and we shall put $V_1 = V_2 = V$, and $\hbar = 1$.

Since the Hamiltonian (2.1) is periodic in time, i.e.,

$$\hat{H}(t+T) = \hat{H}(t), \quad T = 2\pi/\nu, \tag{2.10}$$

the description of the system can be given in terms of the quasienergy functions:[14,15]

$$\psi_\lambda(\theta, t) = e^{-i\lambda t}\varphi_\lambda(\theta, t), \quad \varphi_\lambda(\theta, t+T) = \varphi_\lambda(\theta, t). \tag{2.11}$$

The quantity λ in these expressions is the quasienergy of the system. We now introduce the evolution operator $\hat{S}$ for the wave function during the external field period:

$$\psi(\theta, t+T) = \hat{S}\psi(\theta, t).$$

Let $\psi_\varepsilon(\theta, t)$ be an eigenfunction of the evolution operator $\hat{S}$:

$$\hat{S}\psi_\varepsilon(\theta, t) = e^{-i\varepsilon}\psi_\varepsilon(\theta, t), \tag{2.12}$$

where $\varepsilon = \lambda T$. It will be convenient to refer to ε as the quasienergy.

The problem thus reduces to the determination of the evolution operator $\hat{S}$ acting during the external-field period T, and to the subsequent determination of its eigenfunctions and eigenvalues.

Let us divide the interval T into M equal parts: $\tau = T/M$, and replace the operator $\hat{H}$ in (2.1) with

$$\hat{H} = -\gamma\frac{\partial^2}{\partial\theta^2} + \sum_{j=1}^{M} v_j\delta(t-t_j)\cos\theta, \quad v_j = 2V\tau\cos\nu t_j, \tag{2.13}$$

where $t_j = j\tau$. It can be shown that the approximation (2.13) to the original Hamiltonian (2.1) is equivalent to assuming that, apart from the fundamental harmonic $\cos\nu t$, the perturbation acquires higher harmonics with frequencies $M\nu$, $(M \pm 1)\nu$, $(M \pm 2)\nu$, ... For large values of $M \gg 1$, these harmonics are not in resonance, and their contribution is

small. The accuracy of the calculations is verified in this approach by increasing the parameter M. We usually took $M = 100$ in our numerical experiments.

All this means that the evolution operator $\hat{S} \equiv \hat{S}_{t=0}$ can be written in the following form:

$$\hat{S} = \hat{S}_1 \hat{S}_2 \ldots \hat{S}_j \ldots \hat{S}_{M-1} \hat{S}_M, \tag{2.14}$$

where

$$\hat{S}_j = \exp\left[-i\frac{\tau\gamma}{2}\frac{\partial^2}{\partial\theta^2}\right] \exp[-iv_j \cos\theta] \exp\left[-i\frac{\tau\gamma}{2}\frac{\partial^2}{\partial\theta^2}\right]. \tag{2.15}$$

Since the original Hamiltonian is invariant under a change in the sign of θ, the quasienergy eigenfunctions can be classified in accordance with their parity. To simplify the calculations, we shall confine our attention to antisymmetric functions: $\psi_\varepsilon(-\theta,t) = -\psi_\varepsilon(\theta,t)$. We take as our basis the antisymmetric functions of the unperturbed operator

$$|n\rangle = \pi^{-1/2} \sin n\theta \quad (n=1, 2, \ldots). \tag{2.16}$$

In this representation, the matrix elements of the operator $\hat{S}_j$ have the form

$$S_{nm}(j) \equiv \langle n|\hat{S}_j|m\rangle = e^{i\tau\gamma n^2/2} B_{nm} e^{i\tau\gamma m^2/2}, \tag{2.17}$$

where

$$B_{nm} = \frac{1}{2N+1} \sum_{l=1}^{2N+1} \left[\cos(n-m)\frac{2\pi l}{2N+1} - \cos(n+m)\frac{2\pi l}{2N+1} \right]$$
$$\cdot \exp\left[-iv_j \cos\frac{2\pi l}{2N+1}\right] \quad (n, m=1, \ldots, N). \tag{2.18}$$

The parameter N in (2.18) is equal to the total number of states (2.16) in the numerical experiment. The criterion for choosing N was that the change in the eigenfunctions and eigenvalues in the region of phase space under investigation was small as N was increased (we usually assumed that $N = 89$ or 151).

We note that the matrices $S_{nm}(j)$ in (2.17) are symmetric and unitary. Thus, finally, the matrix S_{nm} obtained by multiplying together the matrices in (2.17) has the same symmetry properties. The symmetry of the unitary matrix S_{nm} signifies that the model with a finite number of levels is invariant under time reversal [in accordance with the properties of the original system (2.1)]. The numerical analysis thus reduces to the determination of the quasienergy spectrum and the quasienergy eigenvalues of the symmetric matrix

$$S_{nm} = \sum_{m_1,\ldots,m_M} S_{nm_1}(1)S_{m_1m_2}(2)\ldots S_{m_M m}(M). \tag{2.19}$$

3. STRUCTURE OF QUASIENERGY FUNCTIONS IN THE CRITICAL REGION ($K \sim 1$)

Let us first consider the properties of the eigenfunctions of an isolated nonlinear resonance, which can be obtained from (2.1) by setting, for example, $V_1 = V$ and $V_2 = 0$. The Hamiltonian of an isolated resonance then assumes the form[12,13]

$$\hat{H} = -\gamma\hbar^2 \frac{\partial^2}{\partial\vartheta^2} + V\cos\vartheta, \tag{3.1}$$

where $\vartheta = \theta + vt$, and we have transformed to the new wave function $\varphi(\vartheta,t)$:

$$\varphi(\vartheta, t) = e^{i(l_i\vartheta - \tau\hbar l_i^2 t)}\Psi(\vartheta, t); \tag{3.2}$$

where l is the number of the resonance level satisfying the condition [see the left-hand inequality in (2.3)]

$$2\gamma\hbar l_i = -v. \tag{3.3}$$

The determination of the eigenfunctions of the Hamiltonian (3.1) reduces to the solution of the Mathieu equation

$$\gamma\hbar^2 \frac{d^2\varphi_\varepsilon(\vartheta)}{d\vartheta^2} + (\varepsilon - V\cos\vartheta)\varphi_\varepsilon(\vartheta) = 0, \quad \varphi_\varepsilon(\vartheta+2\pi) = \varphi_\varepsilon(\vartheta). \tag{3.4}$$

The solutions of this equation are the periodic Mathieu functions, whose Fourier series will, in general, have a relatively complicated structure. The form of these functions is therefore determined numerically. Figure 1 shows the quasienergy eigenfunctions $\varphi_\varepsilon(\vartheta)$ of bound states in the unperturbed basis $(2\pi)^{-1/2} e^{in\vartheta}$. It is clear that the number of eigenstates in the potential well $V\cos\vartheta$ is in good agreement with the quasiclassical estimate (2.7): $\delta n \approx 36$. Numerical data show that, when $\delta n \gg 1$, the structure of the eigenfunctions near the separatrix (edge of the well) becomes significantly more complicated. It is natural to expect that, when the perturbation is present, these eigenfunctions will undergo a greater change, and an irregularity may appear in their structure (see Sec. 4). Above the separatrix ($\varepsilon_l > V$), the quasienergy functions rapidly approach the asymptotic expressions $\sin(l\vartheta)$ and $\cos(l\vartheta)$, which correspond to the two peaks (Fourier amplitudes) $A_{\pm|l|}$ in Fig. 1.

For the qualitative characterization of the structure of the eigenfunctions corresponding to energy levels with $\varepsilon_l < V$, it is convenient to introduce the following quantities:[20]

$$l = 2\left[\sum_{n=-\infty}^{\infty}(n-\bar{n})^2|A_n|^2\right]^{1/2}, \quad \bar{n} = \sum_{n=-\infty}^{\infty} n|A_n|^2. \tag{3.5}$$

where A_n are the coefficients in the expansion of the eigenfunction $\varphi_\varepsilon(\vartheta)$ in terms of the functions $(2\pi)^{-1/2}e^{in\vartheta}$. The
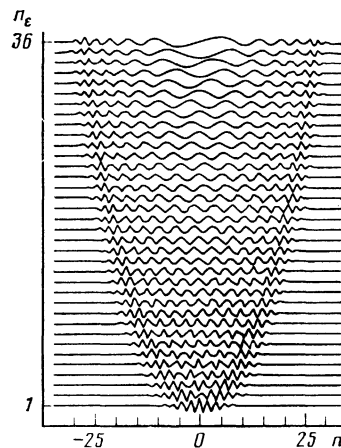

FIG. 1. Quasienergy functions of an isolated resonance in the basis of unperturbed ($V_1 = V_2 = 0$) states. The figure shows the Fourier amplitudes C_n of all the bound-state eigenfunctions ($\varepsilon < V$) of the system defined by (3.4) with $V = 0.2$, $\gamma = 5 \times 10^{-4}$, $\hbar = 1$. The quantity n_ε is the number of the eigenfunction, measured from the bottom of the potential well.
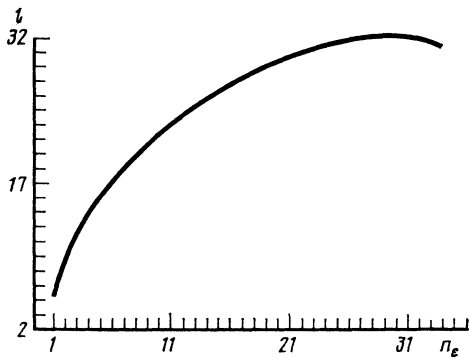
FIG. 2. Root mean square width l [see (3.5)] of an eigenfunction as a function of n_ε for the parameters used in Fig. 1.

FIG. 3. The center of gravity $\bar{n}$ of an eigenfunction as a function of its root mean square width l for the system defined by (2.1) with $V_1 = V_2 = 10$, $\gamma = 5 \times 10^{-2}$, $\delta n \simeq 25.5$. (a) Classical resonances do not overlap, $K \simeq 0.57$, $\nu = 3.5$; (b) strong overlap between resonances, $K \simeq 4.4$, $\nu = 0.45$.

quantity $\bar{n}$ defines the "center of gravity" of the function $\varphi_\varepsilon(\vartheta)$ and l is its root mean square width $(\Sigma_n |A_n|^2 = 1)$. Figure 2 shows l as a function of the number n_ε of eigenstates. It is clear from this figure that the effective width l of the eigenfunction increases as the separatrix (well edge) is approached and, for quasienergy functions lying in the region of the separatrix, $i_s \sim \delta n$ [see, (2.7)].

This delocalization of the quasienergy functions, as the corresponding levels approach the well edge, is a characteristic feature of any undisturbed resonance [including secondary and higher-order resonances of (2.1)]. We therefore have the approximate estimate $l_s^{(m)} \sim \delta n(V_m)$, where V_m is the depth of the potential well for the mth resonance. Since, in the classical case, the quantities V_m are completely determined by the original parameters V, γ, ν, and, according to Refs. 16 and 17, the phase space can be renormalized, the quantities $l_s^{(m)}$ have definite renormalization properties[21] that characterize the quasienergy functions of the quantum-mechanical system.

We now turn to the structure of the quasienergy functions (2.1) for the two interacting resonances in the transition region $K > K_c$, where[16] $K_c \simeq 0.71$, which corresponds to the breaking up of the last invariant rotation curve lying between the classical resonances in (2.2). As noted above, we have confined our analysis to odd quasienergy functions of (2.1) with $V_1 = V_2 = V$, $\hbar = 1$ [here and henceforth, the time dependence of the function $\psi_\varepsilon(\theta,t)$ is not be explicitly indicated]:

$$\psi_\varepsilon(\theta) = -\psi_\varepsilon(-\theta) = \pi^{-1/2} \sum_{n=1}^{\infty} c_n \sin n\theta, \qquad (3.6)$$

where $\psi_\varepsilon(\theta) \equiv \psi_\varepsilon(\theta,0)$. Hence, instead of (3.5), we introduce the following expression:

$$l = 2 \left[\sum_{n=1}^{\infty} (n-\bar{n})^2 |c_n|^2 \right]^{1/2}, \qquad \bar{n} = \sum_{n=1}^{\infty} n |c_n|^2 \qquad (3.7)$$

with the normalization $\Sigma_n |c_n|^2 = 1$.

Figures 3a and b show $\bar{n}$ as a function of l for two values of K, namely, $K \simeq 0.57 < K_c$ (a), which corresponds to weak coupling between the resonances (resonances do not overlap in the classical system) and $K \simeq 4.45$ (b), which is the case of strong coupling (the primary resonances break up in the classical limit). As already noted, further increase in $K > 4.5$ leads to the superposition of the primary resonances and to a reduction in the stochastic component. Each point in Fig. 3
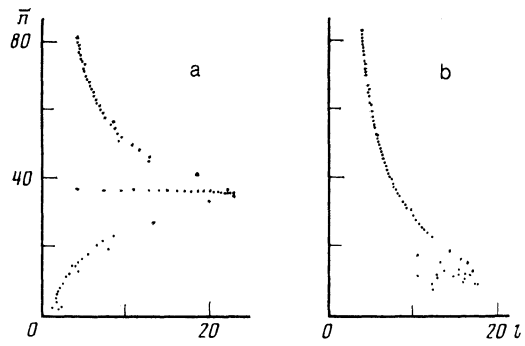
corresponds to an odd quasienergy eigenfunction $\psi_\varepsilon(\theta)$. To compare this with the classical picture of phase space,[16,17] we must augment Fig. 3 with the symmetric lower part $(\bar{n} < 0)$ relative to the line $\bar{n} = 0$. This symmetric picture corresponds to the expansion of $\psi_\varepsilon(\theta)$ in terms of the functions $\exp(in\theta)$. Two symmetric points on the $\bar{n}$, l diagram then determine the same quasienergy function $\psi_\varepsilon(\theta)$ and, in the classical limit, correspond to motion in portions of phase space with $I > 0$ and $I < 0$.

It is clear from Fig. 3a that points corresponding to different $\psi_\varepsilon(\theta)$ are mostly confined to three branches. This picture will now be referred to as a "beak." The upper part of the beak corresponds to functions $\psi_\varepsilon(\theta)$ lying above the edges of the potential wells of the primary resonances (they represent classical trajectories of particles that "pass through"). Points on the horizontal branch of the beak correspond to eigenfunctions of levels inside the potential wells of the primary resonances. The lower branch of the beak in Fig. 3a corresponds to functions $\psi_\varepsilon(\theta)$ lying between the primary resonances and the half-integral resonance on the $\bar{n}$, l diagram (near $\bar{n} \simeq 0$ or $I \simeq 0$ in Refs. 16 and 17). We note two features: (1) points on the horizontal branch with small l correspond to eigenfunctions lying at the bottom of the potential wells of the primary resonances, and such functions are, in this sense, well localized, and (2) the lower branch of the beak in Fig. 3a includes some of the points belonging to the upper branch of the beak for the half-integral resonance (small "burst" near $\bar{n} \simeq 0$ in the lower part of Fig. 3a). The most highly delocalized eigenfunctions corresponding to the neighborhood of the separatrices of the primary resonances are located near the tip of the large beak.

The significant point is that, to each non-broken-up resonance of number m, there corresponds its own mth beak that repeats the basic properties of Fig. 3a but on a smaller scale because the depth of the corresponding potential well decreases with increasing m. Estimates based on the parameters chosen for Fig. 3a show that the number of odd eigenfunctions associated with a half-integer integral resonance is approximately 5, and the resonance is located at the limit of quasiclassical behavior [see (2.9)], so that its beak is partially destroyed.

In the other limiting case of strong coupling (Fig. 3b), the main and half-integral resonances are destroyed and, correspondingly, so is the horizontal branch of the large
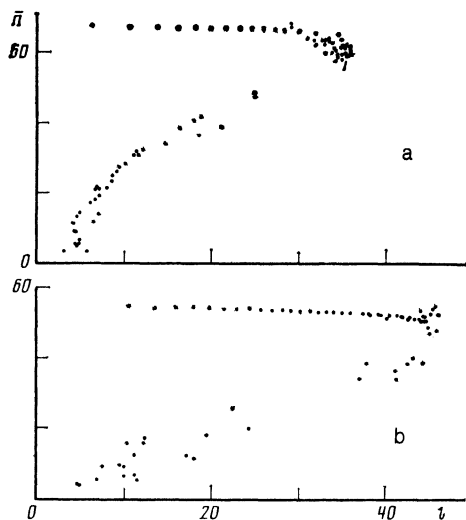
FIG. 4. Breaking up of the lower branch of the beak with increasing overlap parameter K: $\delta n \approx 51$, $V = 20$, $\gamma = 2.5 \times 10^{-2}$. (a) $K = 0.625$, $\nu = 3.2$; (b) $K = 0.8$, $\nu = 2.5$.
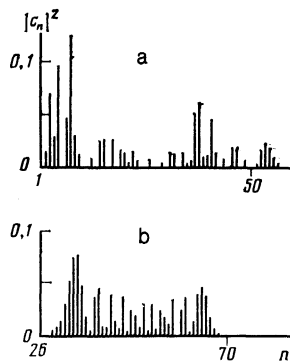

FIG. 5. Example of two quasienergy eigenfunctions in the basis of the unperturbed states for strong overlap between the main resonances of the classical system (2.2): $V_1 = V = 20$, $\gamma = 2.5 \times 10^{-2}$, $K \approx 4.5$, $\nu \approx 0.44$, $\delta n \approx 51$. (a) Eigenfunction from the region of broken-up segments of the beak, $l \approx 36$, $\bar{n} \approx 23$; (b) eigenfunction from the transition region corresponding to the upper branch of the beak, $l \approx 24$, $\bar{n} = 46$.

beak and the entire lower branch. Only the upper branch of the beak, corresponding to high-lying states, remains intact. It is important to note the irregular character of the eigenfunctions belonging to the tip of the large beak that remains intact in Fig. 3b. These functions are not only delocalized (large $l \gg 1$) but, as can be seen from Fig. 3b, the corresponding points are distributed on the $\bar{n}$, l plane in an irregular manner. This means that the very structure of these states must contain a definite fraction of an irregular component. This question will be examined further below.

We now consider the characteristic properties of the destruction of the lower branch of Fig. 3a. This is of particular interest because the destruction of this branch is due to the destruction of the upper branch of the beak corresponding to the half-integral resonance that lies in the region $\bar{n} \approx 0$. In other words, we are concerned with the nature of the breaking up of the eigenfunctions near the separatrix of the half-integral resonance, which, in the classical limit, corresonds to the breaking up of the last invariant curve between the main resonances. Figure 4 shows the breaking up of the lower branch as the overlap parameter K increases (the upper branch is not shown in Fig. 4). It is clear from Fig. 4 that the breaking up of the lower branch occurs because of the breaking up of the half-integral resonance which, moreover, occurs in a irregular manner (lower points in Fig. 4b). As the breaking up proceeds, the eigenfunctions corresponding to the lower branch are rearranged, i.e., they are delocalized (l increases) and are excluded from the region of the tip of the beak corresponding to the primary resonances on the $\bar{n}$, l diagram, where they are also distributed in an irregular manner (the last feature is due to the breaking up of the primary-resonance separatrices). This irregular delocalization of quasienergy functions is the quantum-mechanical manifestation of classical chaos. More detailed properties of the breaking up of the lower branch require further investigation, including the use of larger matrices in the numerical diagonalization of the evolution operator $\hat{S}$.

4. QUASIENERGY FUNCTIONS IN THE REGION OF MAXIMUM CHAOS

We now consider the statistical properties of the quasienergy functions in the region of maximum chaos when the

primary resonances have completely broken up. To do this, we examine the quasienergy functions belonging to the tip of the disintegrated beak. Figure 5 shows the Fourier expansion of two typical quasienergy functions with different localization regions. It is natural to assume that eigenfunctions such as those shown in Fig. 5a, that lie in the stochasticity region produced by the overlap of the two main resonances of the classical system, will have the maximum statistical properties. Points on the $\bar{n}$, l diagram that correspond to these functions are distributed irregularly and belong to the lower, undisturbed part of the beak (Fig. 3b). It may be expected that such states are not only ergodic in the bounded region $1 < n \leqslant n_c$ (Ref. 22), but also have a near-Gaussian distribution[23,24] (see also Ref. 25).

The eigenfunctions were analyzed statistically as follows. The value $n_c = 48$ was chosen so that the localization length of the chosen eigenfunctions was greater than n_c. Next, the interval in n was divided into four equal parts and, for each of them separately, we constructed the histogram of the distributions of the quantity $x_n = \text{Re } c_n$ relative to the mean $\langle x_n \rangle \approx 0$. To improve the statistics, we summed histograms corresponding to different values of the overlap parameter K. As a result, the total number N_1 of realizations on each histogram was $N_1 = 1956$. Figure 6 shows the histogram for $1 \leqslant n \leqslant 12$ (the histograms for the three remaining regions, $13 \leqslant n \leqslant 24$, $25 \leqslant n \leqslant 36$, and $37 \leqslant n \leqslant 48$, are qualitatively similar). The smooth curve in Fig. 6 represents the Gaussian distribution with values of $\langle x \rangle$ and σ determined numerically from the histograms:
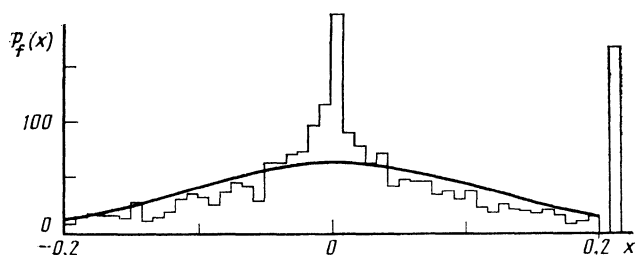

FIG. 6. Histogram of the distribution of the quantity $x_n = \text{Re} C_n$ for eigenfunctions with large localization length $l \gg 1$ and, strong overlap between the resonances: $V = 20$, $\gamma = 2.5 \times 10^{-2}$, $\delta n \approx 51$, $N_1 = 1956$, $n_c = 48$. The overlap parameter was varied in the range $4.5 \leqslant K \leqslant 5.1$. The single separate peak shows the number of values with $|x| > 0.2$.

$$P_f(x) = \frac{N_t}{(2\pi\sigma^2)^{1/2}} \exp\left[-\frac{(x - \langle x \rangle)^2}{2\sigma^2} \right]. \quad (4.1)$$

The data shown in Fig. 6 clearly indicate that $P_f(x)$ is very non-Gaussian. This probably signifies the presence of a regular component in the distribution of the Fourier amplitudes c_n even for states with large localization length $l \gg 1$. It is interesting to note that the distribution $P_f(x)$ is practically independent of the interval over which the summation is carried out. This is somewhat unexpected because it is natural to suppose that, for small n corresponding to the most broken-up region with overlapping resonances in the classical model, the correlation should be lower than that at the edge of localization of the eigenfunction $n \lesssim n_c \ll l$. These numerical data can be interpreted so that the limited size (in terms of action) of the region with stochastic behavior leads to substantial correlation between the amplitudes throughout the eigenfunction localization region. In the final analysis, these correlations enhance the quantum-mechanical limitation of classical chaos (which, in this system, is not highly developed).

5. STATISTICS OF THE QUASIENERGY SPECTRUM

It is well-known that definite statistical properties of the quasienergy spectrum of a quantum-mechanical system can be associated with the chaotic motion of an autonomous classical system (see, for example, Refs. 4 and 26). Different statistical tests[27] are used in quantitative descriptions, including the distribution $P(s)$ of the separation between neighboring energy levels in the spectrum of the system. The function $P(s)$ is an important characteristic of the Wigner-Dyson theory[28,29] in the statistical description of complex quantum-mechanical systems, for example, heavy nuclei and atoms. A simple form is

$$P(s) = As^\beta e^{-Bs^2}, \quad (5.1)$$

where s is the separation between neighboring levels, A, B are normalizing constants, and β is a parameter defining the degree of repulsion between neighboring levels. As reported in Ref. 29, the values $\beta = 1, 2, 4$ are associated with the symmetry of the original system.

It was shown in Refs. 30 and 31 that the Wigner-Dyson distribution (5.1) is also valid for nonautonomous systems (with time-periodic perturbation) that are stochastic in the classical limit (see also Ref. 32). In this case, the function $P(s)$ is the distribution of the separation between neighboring quasienergy levels, reduced to the interval $2\pi/T$, where T is the perturbation period.

For our system, i.e., (2.1), the distribution $P(s)$ has the form shown in Fig. 7a for all quasienergies ε_l and maximum chaos ($K \simeq 4.4$). Here, as before, the statistics was improved by using an ensemble of several matrices (2.19) with different values of the stochasticity parameter K. For comparison, Fig. 7a also shows the Poisson distribution.

$$P(s) = (N_t/\Delta)e^{-s/\Delta}, \quad (5.2)$$

that can describe $P(s)$ with sufficient precision for systems that are integrable in the classical limit (see Ref. 33 and the discussion given in Ref. 34). It is clear from Fig. 7a that the numerical data for $P(s)$ are closer to (5.2) than to the Wigner-Dyson distribution (5.1). We note that, by virtue
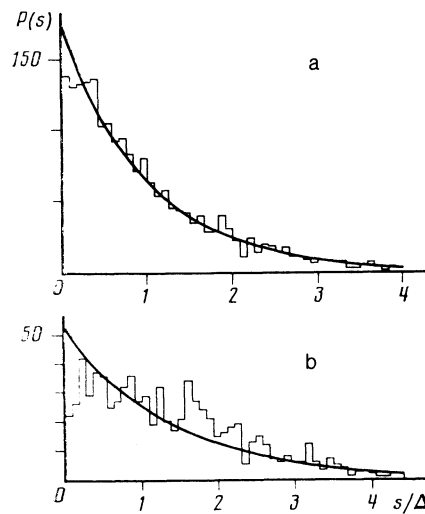

FIG. 7. Distribution $P(s)$ of the separation between neighboring values of quasienergy for $V = 20$, $\gamma = 2.5 \times 10^{-2}$, $\delta n = 51$. The quantity Δ corresponds to the average separation between the levels: $\Delta = 2\pi/N$. Smooth curve—Poisson distribution (5.2); a—the distribution $P(s)$ for all eigenvalues, $N_1 = 2047$, $4.31 \leqslant K \leqslant 4.52$, $0.44 \leqslant v \leqslant 0.46$; b—the distribution $P(s)$ for the most delocalized and irregular states, $N_1 = 778$, $4.31 \leqslant K \leqslant 4.46$, $0.45 \leqslant v \leqslant 0.46$.

of the invariance under time reversal of both the original system (2.1) and the model (2.13)–(2.19), we need only consider $\beta = 1$. Despite the reasonable qualitative agreement between $P(s)$ of Fig. 7a and the Poisson distribution (5.2), there is a significant discrepancy between them for $s \ll \Delta$. The fact $P(s)$ is close to the Poisson distribution is not surprising because the statistical analysis was performed for all the eigenvalues, most of which correspond to highly localized states. The distribution includes states corresponding to stable classical motion outside resonance (rotation). It is therefore natural to consider the statistics of eigenvalues of quasienergy states that have large widths $l \gg 1$ and are irregular to some degree.

Figure 7b shows $P(s)$ for eigenvalues corresponding to the most delocalized quasienergy eigenfunctions (see Sec. 4 and Fig. 6). Comparison with Fig. 7a in the region of small s shows that the discrepancy as compared with (5.2) has become greater. In particular, we note the appearance of repulsion between neighboring quasienergy levels. On the whole, however, the distribution $P(s)$ for these states is very different from the Wigner-Dyson distribution (5.1) with $\beta = 1$. This indicates that there is considerable correlation between the quasienergy states and is in agreement with the Gaussian character of the fluctuations in the eigenfunction components, mentioned in Sec. 4. In this case, the distribution $P(s)$ (Fig. 7b) is intermediate between the Poisson and Wigner-Dyson distributions. This situation is typical for autonomous quantum-mechanical systems whose phase space in the classical limit is split into regions with stable motion and regions in which the motion is stochastic (see, for example, Ref. 35).

6. CONCLUSION

The quasienergy representation is a satisfactory method of describing nonlinear quantum-mechanical systems with an external time-periodic field. On the $\bar{n}$, l plane ($\bar{n}$ is the center of gravity of the quasienergy function and l is its effective width), the quasienergy functions form a charac-

teristic structure when the quasiclassical parameter is large, which we have called the "beak." Since, in the classical limit, a potential well with amplitude V_m corresponds to each isolated resonance, and there is a definite renormalization of phase space due to the higher resonances,[16,17] an analogous renormalization occurs in the quantum-mechanical case on the $\bar{n}$, l plane for beaks corresponding to resonances that remain intact. However, in this picture, there is a quantum-mechanical limit due to the existence of high resonances for which the number of involved levels is low.[21]

It is well-known that, in the classical system, the destruction of the resonances is accompanied by the appearance of regions with a chaotic component. In the first instance, such regions appear in the neighborhood of the separatrices of interacting resonances. The quantum-mechanical case differs from the classical by the absence of the separatrix, i.e., a quantum-mechanical nonlinear resonance, described by (3.4), always has a finite transition region near the edge of the well with $\Delta \varepsilon = \varepsilon_{l+1} - \varepsilon_l \neq 0$. The analog of classical stochasticity in the quantum-mechanical case in the language of quasienergy eigenfunctions is their rearrangement with the appearance of an irregularity on the $\bar{n}$, l diagram, and their delocalization. The latter signifies a significant rearrangement of the quasienergy function due to an increase in the number of unperturbed spectrum harmonics that it contains (see Fig. 5).

The distributions of delocalized quasienergy functions corresponding to broken-up resonance and the distribution of separations between neighboring quasienergy levels show the presence of significant correlations. These are due to the restricted chaotic motion in the phase space of the classical system, as well as, quantum-mechanical effects that restrict classical chaos.

The author is greatly indebted to B. V. Chirikov for his constant interest in this research and for useful suggestions, and to A. R. Kolovskiĭ and D. L. Shepelyanskiĭ for discussions.

^{1}*Rydberg State of Atoms and Molecules* [Russ. transl., Mir., Moscow 1985], ed. by R. F. Stebbings and F. B. Dunning, Cambridge Unversity-Press, 1983.

^{2}N. B. Delone, V. P. Krainov, and D. L. Shepelyanskiĭ, Usp. Fiz. Nauk 140, 355 (1983) [Sov. Usp. 26, 551 (1983)].
^{3}B. V. Chirikov, Phys. Rep. 52, 263 (1979).
^{4}G. M. Zaslavskiĭ, *Stochasticity of Dynamic Systems* [in Russian], Nauka, Moscow, 1985.
^{5}A. J. Lichtenberg and M. A. Lieberman, *Regular and Stochastic Motion* [Russ. Transl., Mir, Moscow, 1984], Springer, 1983.
^{6}B. V. Chirikov, F. M. Izaraĭlev, and D. L. Shepelyansky, Sov. Sci. Rev. 2C, 209 (1981).
^{7}G. P. Berman and A. R. Kolovsky, Physica D 8, 117 (1983).
^{8}G. Casati, B. V. Chirkov, I. Guarneri, and D. L. Shepelyansky, Phys. Rev. Lett. 56, 1437 (1986).
^{9}F. M. Izrailev, Physica D 2, 243 (1981).
^{10}G. P. Berman, G. M. Zaslavskiĭ, and A. R. Kolovskiĭ, Zh. Eksp. Teor. Fiz. 88, 1551 (1985) [Sov. Phys. JETP 61, 925 (1985)].
^{11}F. Doveil, Phys. Rev. Lett. 46, 532 (1981).
^{12}G. P. Berman, G. M. Zaslavskiĭ, and A. R. Kolovskiĭ, Zh. Eksp. Teor. Fiz. 81, 506 (1984) [Sov. Phys. JETP 54, 272 (1984)].
^{13}G. P. Berman, G. M. Zaslavsky, and A. R. Kolovsky, Phys. Lett. A 87, 152 (1982).
^{14}Ya. B. Zel'dovich, Zh. Eksp. Teor. Fiz. 51, 1492 (1966) [Sov. Phys. JETP 24, 1006 (1967)].
^{15}V. I. Ritus, Zh. Eksp. Teor. Fiz. 51, 1544 (1966) [Sov. Phys. JETP 24, 1041 (1967)].
^{16}D. F. Escande and F. Doveil, J. Stat. Phys. 26, 257 (1981).
^{17}D. F. Escande, Phys. Rep. 121, 167 (1985).
^{18}G. P. Berman and G. M. Zaslavsky, Physica A 111, 17 (1982).
^{19}E. V. Shuryak, Zh. Eksp. Teor. Fiz. 71, 2039 (1976) [Sov. Phys. JETP 44, 1070 (1976)].
^{20}M. Toda, Phys. Lett. A 110, 235 (1985).
^{21}G. P. Berman, O. F. Vlasova, F. M. Izrailev, and A. R. Kolovskiĭ, Preprint IF SO AN SSSR No. 402F [in Russian], Krasnoyarsk, 1986.
^{22}A. I. Shnirel'man, Usp. Mat. Nauk 29, 181 (1974).
^{23}C. E. Porter and R. G. Tomas, in: *Statistical Theories of Spectra:Fluctuations*, Academic Press, N.Y.-London, 1965 p. 167.
^{24}M. V. Berry, J. Phys. A: Math. Gen. 10, 2083 (1977).
^{25}B. V. Chirikov, Phys. Lett. A 108, 68 (1985).
^{26}O. Bohigas and M. J. Giannoni, Lecture Notes in Physics 209, 1 (1984).
^{27}T. A. Brody, J. Flores, J. B. French, P. A. Mello, A. Pandey, and S. S. Wong, Rev. Mod. Phys. 53, 385 (1981).
^{28}E. P. Wigner, in: Statistical Theories of Spectra: *Fluctuations, Academic Press*, N.Y.-London, 1965, pp. 88, 145, 176, 226.
^{29}F. J. Dyson, J. Math. Phys. 3, 140, 157, 166 (1962).
^{30}F. M. Izraĭlev, Preprint IYF SO AN SSSR No. 84–63, Novosibirsk, 1984.
^{31}F. M. Izraĭlev, Phys. Rev. Lett. 56, 541 (1986).
^{32}J. V. Jose and R. Cordery, Phys. Rev. Lett. 56, 290 (1986).
^{33}M. V. Berry and M. Tabor, Proc. R. Soc. London Ser. A Math. Phys. Sci. 356, 375 (1977).
^{34}G. Casati, B. V. Chirikov, and I. Guarneri, Phys. Rev. Lett. 54, 1350 (1985).
^{35}T. N. Seligman, J. J. M. Verbaarshot, and M. R. Zirnbauer, Phys. Rev. Lett. 53, 215 (1984); J. Phys. A: Math. Gen. 18, 2751 (1985).